Sounding Rocket Flight Vibration versus Reynold's and Strouhal Numbers

Ricky Wayne Stanfield, Ph.D.
Corvid Technologies, LLC, Mooresville, NC
University of Maryland Eastern Shore, Princess Anne, MD

Abstract

The flight vibration environment for sounding rocket class vehicles has been characterized using several approaches through the years. From the mid 1970's to early 2000's, the environments were based on NASA hand-calculated power spectral density data on a limited set of flight vibration measurements. Between 2002 to 2019, work was performed to trend flight vibration environments against common flight analysis parameters such as flight dynamic pressure and Reynold's number over a much wider set of data. More recently, an exploration was started with several new sounding rockets data sets to determine the extent to which the vector components of flow velocity across the diameter of the rocket generate certain vibration features. This crossflow is caused by small airframe flight path angles of attack and contributes to vibration features that do not otherwise follow the larger trend with Reynold's number. In this paper, we discuss the empirical correlation between flight vibration magnitude and spectral content to Reynold's Number and Dynamic Pressure; the correlation of some vibration features with airframe angle of attack, crossflow velocity, and Strouhal number; and how other interactions between structural frequencies and aerodynamically driven vortex shedding frequencies generate transient vibratory features.

Introduction

The sounding rocket community has been analyzing the flight performance of sounding rocket vehicles since the 1960's. By the 1990's the flight analysis process had been distilled down to an efficient set of standardized parameters and plots that fully captured and characterized the flight performance and stability of these vehicles. Of the many important parameters used to define the performance of a sounding rocket, one key and recurring parameter is Dynamic Pressure (Q). Q was used in early trending of vibration levels as a function of flight time. However, another key parameter is Reynold's Number (Re) which was not commonly plotted in flight performance assessments and so its similarity to Q as a function of time history was not immediately recognized.

Around 2002, we began analyzing flight vibration environments in sounding rocket vehicles in greater detail than previously. This involved a closer look at time domain flight vibration data, spectrogram data, and the corresponding root mean square acceleration (gRMS) as a function of time. About 2005 we noted and paid more attention to similarities between the shape of the flight vibration time domain data and resulting the gRMS vibration magnitude data to Q as a function of time. In more recent studies we finally recognized that Re varies in a similar manner to Q, yet is better correlated with the gRMS vibration magnitude. The trend between gRMS levels and Re was good, but still seemed to lack the ability to match smaller perturbations in gRMS vibration levels. This was initially written off as randomness inherent in the vibration environments. More recently, means were sought to account for contributions from flight path Angle of Attack (AoA), Length/Diameter ratio (L/D), winds aloft, and day of flight atmospheric conditions.

This paper shows the trend of flight vibration gRMS levels with an "enhanced" Re for a selected sounding rocket mission. It recaps how vibration gRMS levels are computed. It describes how AoA, Length to Diameter (L/D) ratio, winds aloft, and atmosphere are introduced into the Re calculations. The paper shows the improved alignment of gRMS vibration levels to the enhanced Re values. Finally, the paper discusses the use of the resulting proportionality constants to estimate gRMS for a future sounding rocket flight based on predicted Re profiles. Mention is made of how Strouhal number (St), Helmholtz resonation, and other structure borne vibrations are related to the frequency content within frequency spectrum that underlies the gRMS vibration envelope.

DFARS 252.235-7010 Acknowledgment of Support and Disclaimer (MAY 1995). (a) This material is based upon work supported by the Naval Surface Warfare Center – Port Hueneme Division (NSWC PHD) Contracting Office under Contract No. N00178-19-D-5001. (b) The opinions, findings, conclusions, and recommendations expressed in this material are those of the authors and do not necessarily reflect the views of the NSWC PHD Contracting.

Computing gRMS History

As a recap of prior work in determining the gRMS level as a function of time, consider the following sequence of figures. The sounding rocket is fitted with AC-coupled accelerometers (vibrometers) with suitable dynamic range, analog low-pass filters, and sufficient data sampling rate to capture vibration without the influence of gravity, vehicle acceleration, or signal aliasing. Telemetered data is recorded on the ground. The recorded data is later processed to remove telemetry drop-outs, time-stamp issues, and DC bias offsets or drift. This results in a clean time domain signal suitable for digital signal processing.

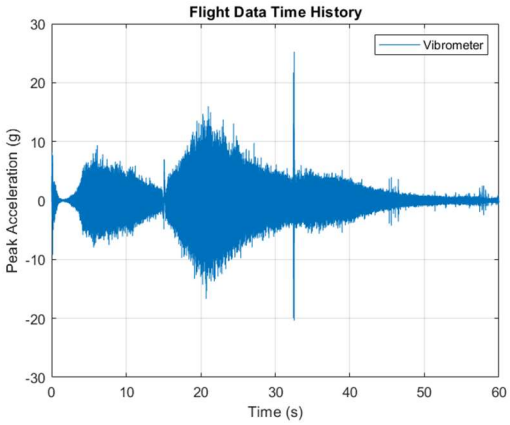

Figure 1. Time Domain

The cleaned time domain signal is then processed in one-second data segments based on sampling rate, with a 90% overlap. Each sample is processed using an n-point Fast Fourier Transform (FFT) when n is the integer sampling rate. The FFT is then used to compute a Power Spectral Density (PSD) for that moment in time. The resulting PSD has a frequency resolution of 1 Hz. In general, frequency resolution less than 1 Hz has not been more informative, though recent control system applications may benefit from ½ Hz resolution. Wider frequency resolution for looking at spectra, which includes fractional octave band approaches, will mask or hide important narrow band features. Spectral smoothing techniques such as Welch's method or swept averaging will also suppress narrow band frequency domain features. Smoother PSD results can be useful for defining test spectra. In this analysis, these fine frequency domain features are important and should be preserved.

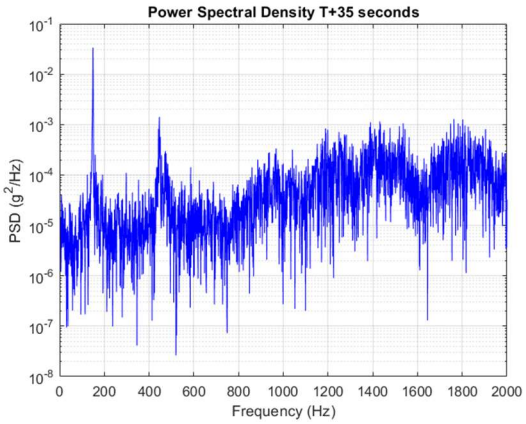

Figure 2. Power Spectral Density

The set of PSDs with that 90% overlap are arranged side-by-side. This forms a spectrogram plot that has 0.1 second time axis resolution and 1 Hz frequency resolution. Because of the time segment overlapping, short duration transient events such as a mechanical shock event will blur or bleed across up to ten adjacent time slices. However, this is generally not an issue for data interpretation. The benefit of the spectrogram is that it shows frequency content and change in the signal as a function of time. Flight vibration is not a "stationary" process. That is to say the signal magnitude and its frequency content is changing constantly. No single PSD cross section of the spectrogram is representative of the entire flight. Spectrogram help visualize the change with time.

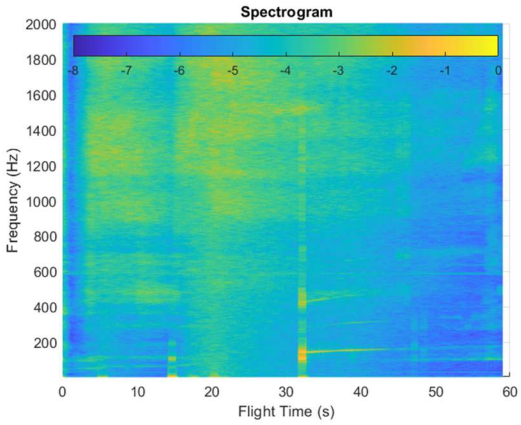

Figure 3. Spectrogram

It is useful to view PSDs in a semilog-y format for consistency with spectrogram plots. PSD plots in

DFARS 252.235-7010 Acknowledgment of Support and Disclaimer (MAY 1995). (a) This material is based upon work supported by the Naval Surface Warfare Center – Port Hueneme Division (NSWC PHD) Contracting Office under Contract No. N00178-19-D-5001. (b) The opinions, findings, conclusions, and recommendations expressed in this material are those of the authors and do not necessarily reflect the views of the NSWC PHD Contracting.

log-log format are common in test specification documents and references, but logarithmic frequency axes in spectrograms are difficult to interpret, especially at mid to high frequencies where more flow induced vibration is found.

Each vertical cross section of the spectrogram is the underlying PSD. The gRMS area under each of those vertical PSD profiles is computed and then used to generate a gRMS magnitude history. Since the frequency resolution of the PSD is 1 Hz, the gRMS area is simply the square root of the sum of the PSD magnitude in each frequency bin across the desired bandwidth. The gRMS is sensitive to the considered bandwidth. In this case the gRMS magnitude is computed between 5 Hz and 2000 Hz. There is certainly more vibration energy in the time domain signal and the PSD plot above 2000 Hz. The use of the 2000 Hz upper frequency limit is loosely based on the associated amount of physical displacement and the potential of that displacement to cause damage. Between the spectrogram and gRMS history, a full and complete definition of the flight vibration environment is generated; total magnitude and frequency content.

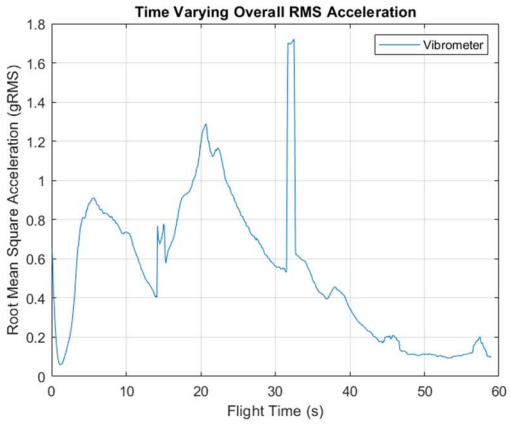

Figure 4. gRMS History

Velocity, AoA, L/D, Winds, and Atmosphere

With the flight vibration history computed and defined, the associated flight trajectory environment and atmospheric conditions need to be collected so that the instantaneous Re can be accurately estimated. As described in many references, Re is the ratio of inertial forces and viscous forces within a fluid subjected to relative fluid movement at different velocities. The expression for Reynold's Number is

$$Re = \frac{\rho u L}{\mu}$$

where:

- ρ is the density of the fluid
- u is the velocity of the fluid
- L is the characteristic length
- μ is the dynamic viscosity of the fluid

Values for air density vary as a function of altitude. Air density, temperature, and viscosity also vary as a function altitude. Vehicle altitude obviously varies as a function of time. The characteristic length and diameter of the vehicle varies as a function of vehicle staging. Vehicle total velocity, flight AoA, and the associated cross-axis flow of air vary as a function of time. All of these quantities need to be determined and woven together to compute the most correct value of Re at each moment of time.

During boost, both vehicle velocity and altitude are increasing, while air density, air static pressure, and air temperature are decreasing. These changing quantities result in the associated Mach number (M) over time. The vehicle in this case spends time in the transonic region between 0.8 M and 1.2 M which is a typically turbulent flight regime.

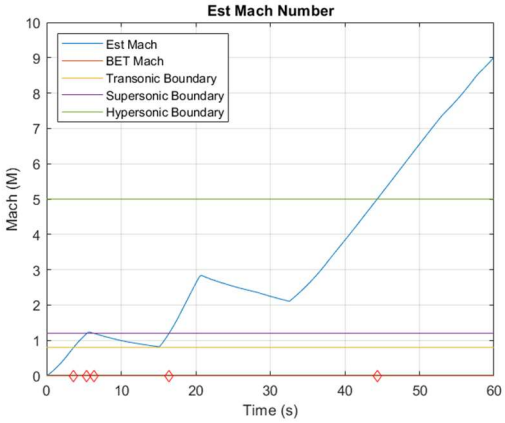

Figure 5. Mach Number

In this flight, that period of time included the motor staging event, some velocity reduction during the coast, and changes in AoA magnitudes. Beyond 16 seconds it is smoothly supersonic and hypersonic.

DFARS 252.235-7010 Acknowledgment of Support and Disclaimer (MAY 1995). (a) This material is based upon work supported by the Naval Surface Warfare Center – Port Hueneme Division (NSWC PHD) Contracting Office under Contract No. N00178-19-D-5001. (b) The opinions, findings, conclusions, and recommendations expressed in this material are those of the authors and do not necessarily reflect the views of the NSWC PHD Contracting.

Ideally, the vehicle would fly with a perfectly straight attitude relative to the velocity vector throughout its trajectory, but inevitably it will develop some AoA relative to its velocity vector. AoA changes based on the body dynamics, roll rate, and stability margins of the vehicle. In this mission, AoA fluctuated a fair amount during the coast period mentioned above. There was a large AoA during the coast between the second and third stage. AoA can be thought of as splitting the airflow across the vehicle airframe into two main components; A longitudinal component of velocity and a crossflow component of velocity. A Re value for each component of velocity and using the appropriate characteristics diameter or length can be computed for each moment of flight time.

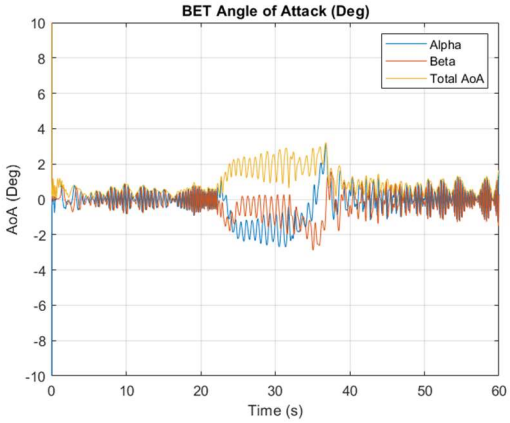

Figure 6. Angle of Attack

Since AoA is small, the longitudinal component of velocity is almost indistinguishable from the vehicle total velocity. The crossflow velocity is also small, but it is not insignificant, it is sub-sonic, and it is influential in the vibration results for the flight. The longitudinal flow and the crossflow velocities can be recombined using the Root Sum Squared (RSS) method to recover the original total vehicle velocity. The same RSS vector sum can be performed on the two Re values for the longitudinal flow and the crossflow. It will be shown that doing this generates an AoA dependent variation in the instantaneous Re values that cannot otherwise be generated using the bulk velocity of the vehicle and a single characteristic dimension alone. When this RSS Re value is combined with other day of flight atmospheric factors the result is a more dynamic and enhanced Re value.

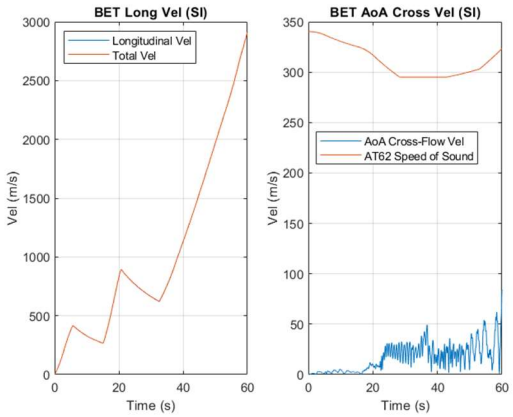

Figure 7. Components of Velocity

In addition to the AoA induced crossflow velocity, the vehicle passes through wind layers as a function of altitude, which are also a component of crossflow velocity. The flight path may not always be truly perpendicular to the winds aloft, but for this analysis that is assumed. Meteorological (MET) balloon data sets are collected in the hours prior to the flight. They are used to determine the mean wind velocity and direction. They also measure actual Day of Flight (DoF) atmospheric properties including air density and air temperature. These can be compared to the 1962 Standard Atmosphere (AT62) properties. In some cases, the MET balloon data is perfectly aligned with the AT62 standard atmosphere. In other instances, air density and air temperature can be dramatically different than AT62. When available, the balloon MET Data will provide a much better estimate of Re, though certainly the AT62 data is good for when no MET data is accessible or for when vibration predictions are made for a future flight. It is recognize that there are other atmosphere models other than the AT62 model, but that is the default model built into this analysis.

DoF wind speed can be compared to historical winds for the launch site. For winds above the highest balloon measurement altitude an exponential decay of wind speed can be assumed, since by those high altitudes the values of Q and Re are already negligibly small. Wind direction is important for trajectory analysis, but appears less important to vibration analysis. Since sounding rockets are rolling about their long axis during flight at a given roll rate, the influence of wind direction on vibration is likely

DFARS 252.235-7010 Acknowledgment of Support and Disclaimer (MAY 1995). (a) This material is based upon work supported by the Naval Surface Warfare Center – Port Hueneme Division (NSWC PHD) Contracting Office under Contract No. N00178-19-D-5001. (b) The opinions, findings, conclusions, and recommendations expressed in this material are those of the authors and do not necessarily reflect the views of the NSWC PHD Contracting.

evenly distributed across the airframe. There is little evidence at this point that the winds aloft direction has any influence on flight vibration levels, so it is not accounting for in this analysis. In this flight, there was a strong wind velocity component between 30Kft and 40Kft associated with the jet stream. This is common. High level winds were strong too, but are in much thinner and less influential air densities.

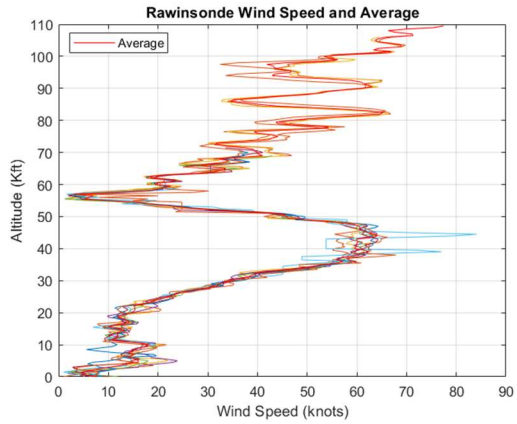

Figure 8. Day of Flight Average Winds

The vertical DoF cross wind profile data can be interpolated base on vehicle trajectory altitude versus time data (which was not plotted for this report) to determine the cross wind speeds as a function time and altitude for the vehicle.

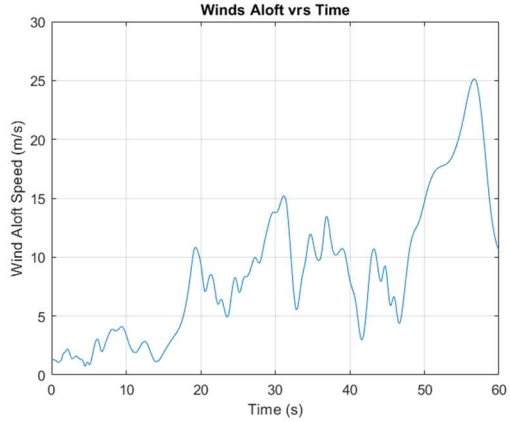

Figure 9. DoF Winds versus Flight Time

This wind speed component as a function of time is assumed to be perpendicular to the flight path and is added to AoA induced cross axis velocity to arrive at a total cross flow velocity. Total cross flow velocity is shown in yellow in the plot below and used for the enhanced Re calculations. Cross flow velocity for this mission remained subsonic, but in other missions that have been evaluated, the cross flow velocity did approach supersonic speeds.

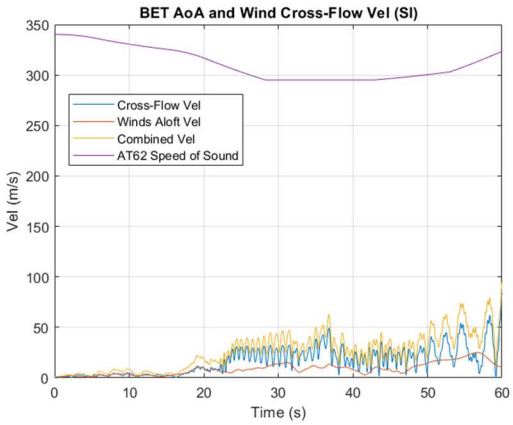

Figure 10. Total AoA-DoF Wind Cross Velocity

DoF air density for this flight and in general is not too different than the AT62 data. However, since air density is a major contributor to Re calculations, even this small deviation from the AT62 standard is influential.

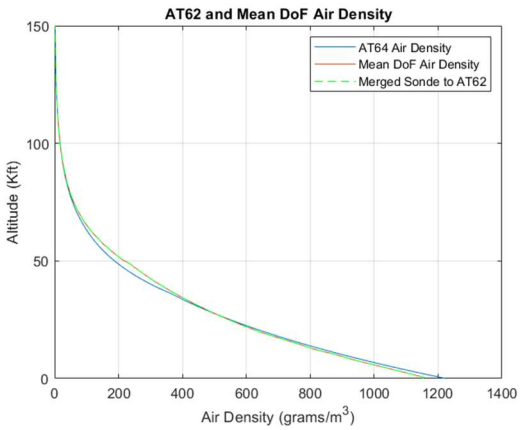

Figure 11. Day of Flight Air Density

DoF air temperature can be very different than the AT62 model. Air temperature impacts air density and viscosity, but it is a smaller influencer on Re than is air density. However, there are clear signs of the impact of air temperature on the match between Re values and the resulting vibration levels.

DFARS 252.235-7010 Acknowledgment of Support and Disclaimer (MAY 1995). (a) This material is based upon work supported by the Naval Surface Warfare Center – Port Hueneme Division (NSWC PHD) Contracting Office under Contract No. N00178-19-D-5001. (b) The opinions, findings, conclusions, and recommendations expressed in this material are those of the authors and do not necessarily reflect the views of the NSWC PHD Contracting.

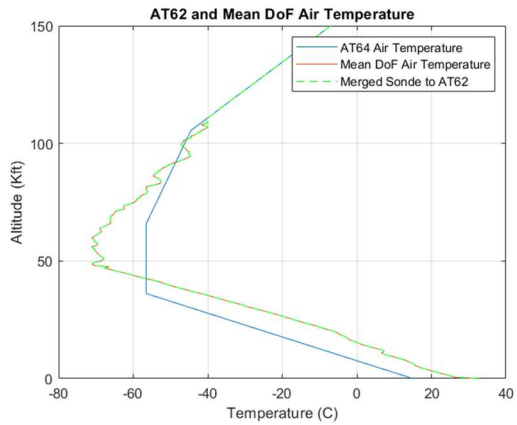

Figure 12. Day of Flight Temperature

As was done with the wind data, the vertical profiles for DoF air density and air temperature can be interpolated based on trajectory attitude versus time data in order to determine their values for each moment in the time of flight. This enables their values to be properly included in the instantaneous and enhanced Re calculations.

During earlier analyses when the longitudinal and cross axis flows were not being separated, the characteristic length was taken to be the payload diameter. This was done because sounding rocket diameters are more consistent mission to mission, whereas vehicle lengths tended to range widely and even change during flight. This allowed the comparison of gRMS/Re results across many missions. Now in this analysis, the air flow is being separated into the longitudinal flow and cross flow components, and a Re value for each of these flows is to be computed. It is now more important that the right characteristic dimension be applied to the Re calculations.

In the longitudinal flow direction of the vehicle, the characteristic dimension is taken to be the payload diameter. This seems counter-intuitive since overall vehicle length would seem to be the more logically associated dimension to longitudinal flow. However, in sensitivity tests using length and diameter with the longitudinal and cross flows, the combination of diameter and longitudinal flow velocity along with length and cross flow velocity provided the best alignment between resulting enhanced Re data and gRMS data. This may be more related to the characteristic dimension of the presented cross section of the vehicle to the flow direction, than it is to the dimension of the vehicle in the flow direction. The characteristic diameter is assumed to be constant at the value of the payload diameter since the change in diameter for each stage is negligibly small.

For the vehicle cross flow direction, the characteristic dimension is taken to be the payload length. In this analysis, the vehicle characteristic length changes at each staging event when the spent rocket motors drop away. Therefore, at different points in the analysis the effective Length to Diameter (L/D) ratio value is adjusted.

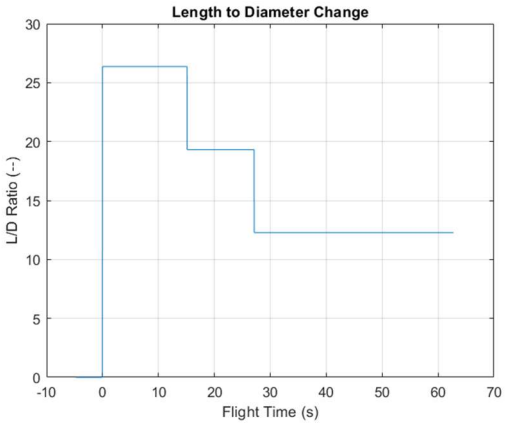

Figure 13. L/D Change with Staging

The nominal Re value associated with the long axis component of velocity for each moment of time is computed separately from the nominal Re value associated with the cross-axis component of velocity. The wind velocity is added to the crossflow velocity. DoF atmospheric air density and air temperature are applied for each moment of time. The appropriate characteristic dimension values for the time of flight are applied. Once the two individual nominal Re values are determined, the enhanced Re RSS vector sum is computed. This enhanced Re value is used in the trending with gRMS levels.

To illustrate these calculations, consider first the Re values when the nominal total velocity of the vehicle is used to compute them using the AT62 and the DoF atmosphere without any separation of the cross flow. The nominal Re as a function of time using the AT62 atmosphere and total vehicle velocity is shown in blue. The value of Re using the DoF air properties is

shown in red. The DoF air density differences pull down Re values during early flight and then increases the Re values for the latter part of flight. In addition, the ripples in the DoF air temperature profile add some small ripples to Re, most visible around 35 seconds.

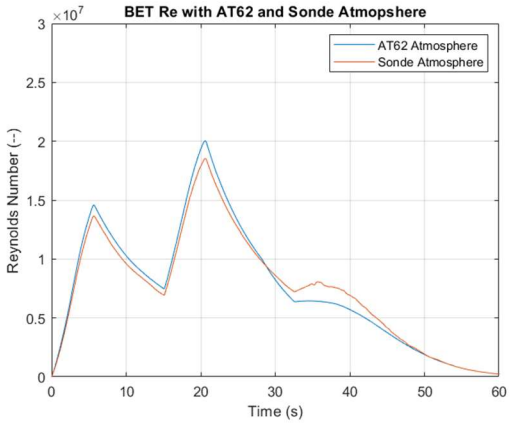

Figure 14. Default Re for AT62 and DoF

Next, the influences of the AoA induced cross flow are included. The nominal Re value is again shown in blue. The longitudinal component of Re (based on characteristic diameter) is shown in dotted red, and is largely identical to the nominal Re profile. However, the cross flow component of Re (based on the characteristic length and essentially accounting for the L/D ratio of the vehicle) in yellow is significant and much more variable. When the dotted red and yellow profiles are RSS summed together for each moment of time, the total and enhanced instantaneous Re values emerge, shown in purple.

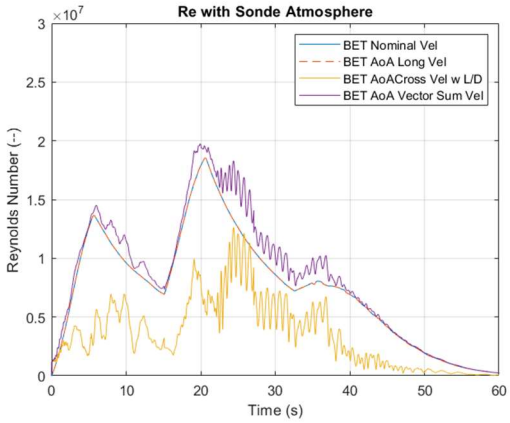

Figure 14. Long, Cross, and Vector Sum Re

To simplify these enhanced Re results a little further, the figure below shows the enhanced Re estimate for this vehicle trajectory for both the nominal AT62 standard atmosphere and the DoF balloon MET atmosphere. The combination of the AoA driven cross flow velocity and the DoF atmosphere results in more representative Re values through which the vehicle flew. The next exercise then is to associate this enhanced Re history with the gRMS history computed earlier.

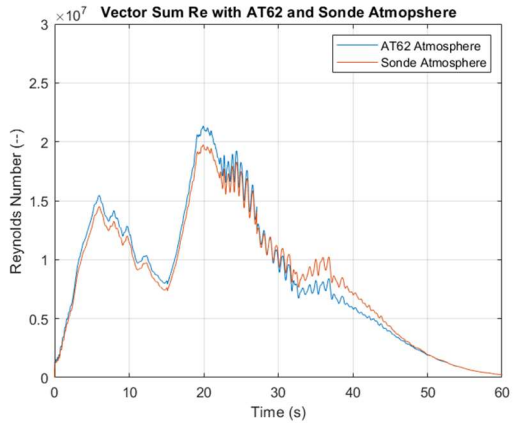

Figure 15. Enhanced Re Estimate

gRMS to Improved Re Trend

The gRMS vibration magnitude history for this mission is repeated here, but this time including a second orthogonal vibration data channel. Both of these vibration measurements were made by a three-axis vibrometer mounted directly to the payload skin wall. The channel in blue was oriented in the long axis of the vehicle which is often referred to at the thrust axis. The channel in orange was mounted radially and is commonly referred to as the lateral axis. The third axis was not recorded. In general, wall-mounted vibrometer lateral vibration levels are greater than for thrust axis vibration. Vibrometers mounted to internal structures will experience an amplification or attenuation of their response based on the Frequency Response Function (FRF) or "transfer function" of that structure. Therefore, these wall mounted measurements show a better agreement between gRMS magnitude and Re, than do some internally mounted sensors.

DFARS 252.235-7010 Acknowledgment of Support and Disclaimer (MAY 1995). (a) This material is based upon work supported by the Naval Surface Warfare Center – Port Hueneme Division (NSWC PHD) Contracting Office under Contract No. N00178-19-D-5001. (b) The opinions, findings, conclusions, and recommendations expressed in this material are those of the authors and do not necessarily reflect the views of the NSWC PHD Contracting.

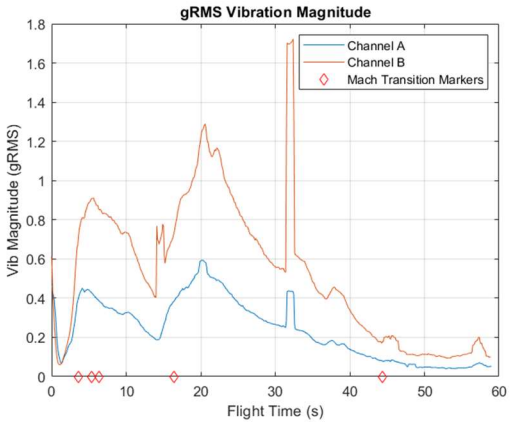

Figure 16. Thrust and Lateral gRMS Vibration

Note the fluctuations of gRMS vibration magnitude as a function of time. There is a large main pattern of magnitude that one might easily see as following the nominal Re profiles shown earlier. There is also a smaller level of fluctuation over time that one might see as related to the cross flow Re as was discussed. To further build on this comparison, compare the two gRMS vibration magnitudes with the enhanced and nominal Re history. Large and small variations in both profiles can be more easily identified. The vector sum Re in orange had some fast oscillations between 20 and 30 seconds associated with the surge in AoA, but that did not seem to translate directly into measured vibration.

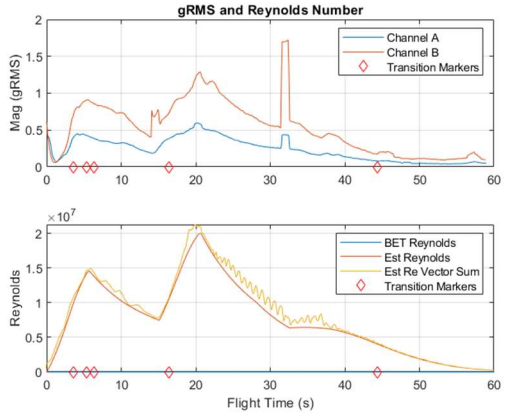

Figure 17. gRMS Vibration and Enhanced Re

To further quantify the relationship between gRMS vibration magnitude and enhanced Re, the ratio of the two quantities can be computed for each moment of time and plotted as shown below in blue. There is a clear linear trend between the two. The large and small variation in the Re levels show as wiggles in the blue line, but they drift up and right with the overall trend. To quantify the trend, a Least Mean Square (LMS) linear regression is computed and shown in the dotted black line. In addition, a Zero y-intercept LMS (ZLMS) regression is also computed. This essentially forces the curve fit to pass through the origin of the plot. When there is no velocity and no Re then there is no vibration, which makes the ZLMS a more valid fit. In most cases the LMS and ZLMS lines are very close to each other. The LMS and ZLMS fits tend to look through the transient fluctuations of data.

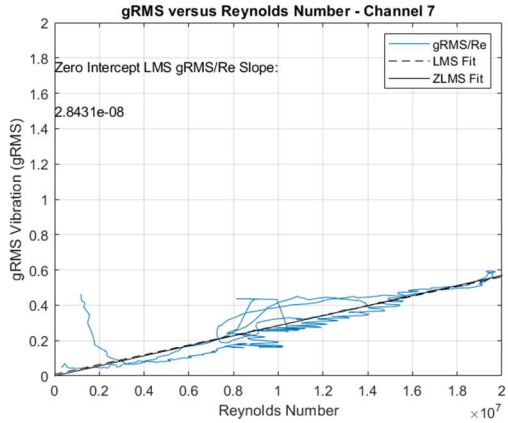

Figure 18. gRMS/Re Ratio and Trend

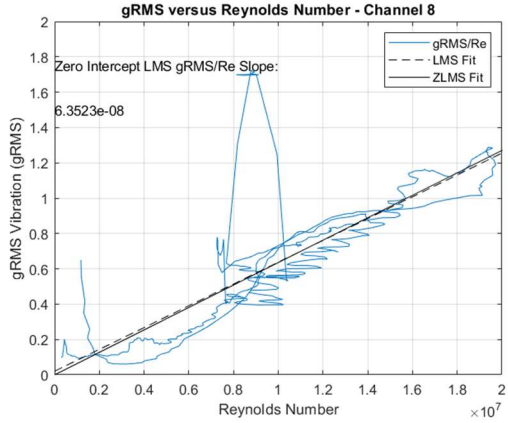

Figure 19. gRMS/Re Ratio and Trend

The ZLMS regression for "Channel 7"has a slope of 2.8431×10^{8} gRMS per unit Re. The slope of the

ZLMS regression for "Channel 8 is 6.3523×10^8 gRMS/Re. Other channels of data for this mission had similar slope which will be discussed presently. In general, the lateral channels have a steeper slope since they show a greater response per unit Re than do the thrust axis responses. The scatter of gRMS versus Re is "fuzzier" for data captured on internal structures. This is because the local FRF or "transfer function" of the internal structure mechanically filters the input from the air flow on the skin of the rocket before it reaches the sensor. The ZLMS slope is a proportionality constant between the aerodynamically induced gRMS vibration level and the instantaneous Re that existed at the time. Instantaneous enhanced Re captures vehicle AoA, velocity, L/D proportions, and the DoF atmospheric properties as a function of time and altitude. It is as tight a correlation as has been documents in sounding rockets analyses to date.

gRMS Predictions

The gRMS/Re proportionality constant can be used to reconstruct the probable gRMS history for the flight. This is done by multiplying the proportionality constant by the enhanced Re vector values for all points of time. Both the ZLMS and LMS constants are used as shown in red and orange in the figures. Because the slopes in these examples are so close, the two estimated gRMS profiles overlap. Estimated gRMS levels not only match the main rise and fall of the measured gRMS vibration data, but they also predict the smaller undulations in the measured data. This was not possible in prior analysis when nominal Re was computed based on a constant characteristic diameter, the AT62 standard atmosphere, and when the air flow velocity was not separated into longitudinal and cross flows using the AoA data.

The match between the measured gRMS vibration levels and the predicted gRMS vibration levels using the instantaneous enhanced Re and gRMS/Re ratio constants is excellent for skin mounted vibrometer data and still good for internally mounted sensors. For internal vibrometers, the proportionality constant tends to be consistent with results for skin mounted sensors on the same mission. Conjecture is that the estimated gRMS level based on the proportionality constant for that location is representative of the vibration levels that would have been measured "on the skin wall" adjacent to the sensor before any mechanical structural filtering happens. An example of this is shown for this reference sounding rocket mission.

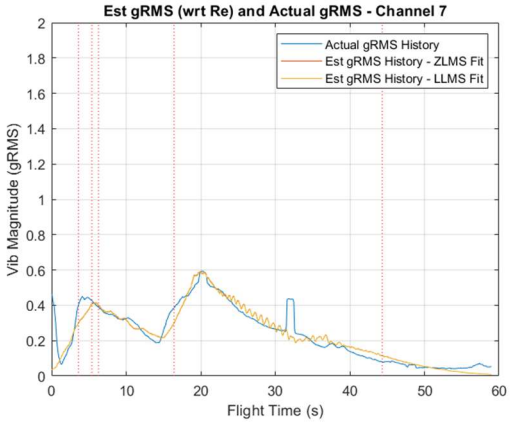

Figure 20. Predicted gRMS wrt Enhance Re

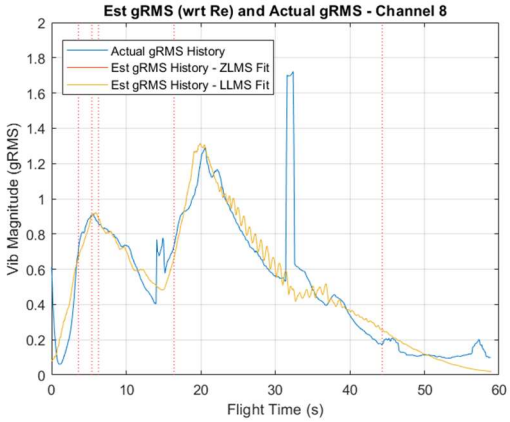

Figure 21. Predicted gRMS wrt Enhance Re

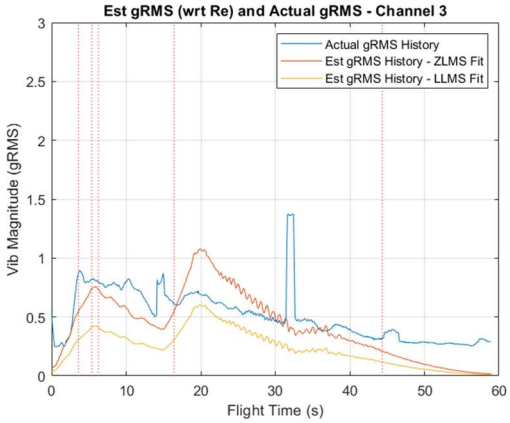

Figure 22. Predicted gRMS wrt Enhance Re

DFARS 252.235-7010 Acknowledgment of Support and Disclaimer (MAY 1995). (a) This material is based upon work supported by the Naval Surface Warfare Center – Port Hueneme Division (NSWC PHD) Contracting Office under Contract No. N00178-19-D-5001. (b) The opinions, findings, conclusions, and recommendations expressed in this material are those of the authors and do not necessarily reflect the views of the NSWC PHD Contracting.

Strouhal and Helmholtz and Motor Specific

There are areas where the estimated gRMS vibration levels do not match the data. The most easily explained examples are the motor ignition shock transients at 18 seconds and 32 seconds. Mechanical shock events generate a sharp broad band PSD spectral response which has a large gRMS area beneath it. Those events are independent of Re. Other deviations have to do with the combustion chamber vibration dynamics from the various rocket motors during the burn. These tend to be strongest early in the motor burn times and comparatively low frequency; less than 300 Hz. Motor combustion noise is also independent of Re. In some missions, the motor related vibration is swamped or masked by the broad band aerodynamic flow induced vibration that was occurring at the same time of flight. Other times, when the air flow is very smooth and quiet, the motor vibration contributions are more noticeable. The last area of mismatch has to do with transient aero-acoustic features that are largely independent of Re. These include "whistling" or "humming" tones, and "chirps" and "groans" from the payload. Consider the trapped volume of air within the payload. That air is venting through small orifices to the outside atmosphere as the vehicle ascents and the outside air pressure is quickly dropping. This can set up a Helmholtz resonator condition that will "hum" at a given frequency, much like blowing across the top of a glass soda bottle. That frequency will shift as a function of flow velocity and atmospheric conditions, but will likely only exist for a short period of time when the conditions are exactly right. Coincidentally, the flight vibration data can be converted into sound since the vibration is in an audible range. These humming features can be heard in some instances which corroborate the theory.

The gRMS vibration magnitude prediction process describe here cannot estimate vibration frequency content, but only the gRMS area under that spectrum. There are two means under exploration for translating the gRMS levels into the underlying spectrum. The first uses the relationship between Strouhal number and Reynold number to estimate the characteristic frequencies of vibration. Initial work has begun to relate the two quantities in the context of these sounding rocket flights. That work is in its infancy and there are no meaningful results to share yet.

The second approach to reconstructing spectrum has two steps. The initial step is to take a composite spectrogram for sets of similar missions to determine the most probable frequency content for a given rocket motor stage of vehicle. This is shown in the figure below. Then the composite spectrogram is re-scaled such that the individual vertical PSD spectral lines of the spectrogram are adjusted up or down in level such that the gRMS area under them matches the predicted gRMS level. From this, maximum and average composed PSD levels can be extracted. This method is working and seems promising. It is mentioned here for awareness, but the details are beyond the scope of this paper.

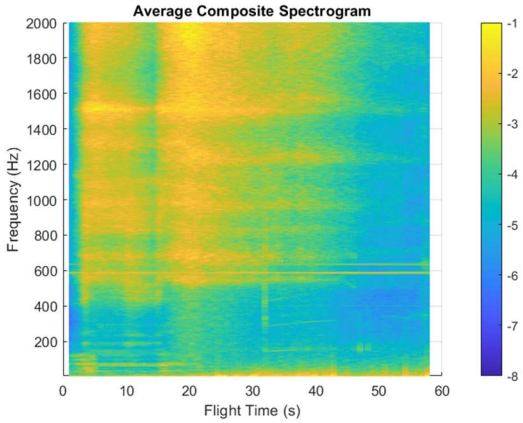

Figure 23. Composite Spectrogram

Trend Across Other Vehicles

In the larger picture, the hypothesis is that the gRMS/Re proportionality constant for the channels of a given sounding rocket mission will be consistent with the ratios from other sounding rocket missions that have similar dimensions, mechanical/structural design approaches, and flight trajectories. If so, then a generalized gRMS/Re constant could be used with the estimated Re profile for a future mission to predict the bulk gRMS vibration magnitudes of that future flight, even if that specific sounding rocket configuration has not been flown before.

Consider all the gRMS/Re ratios for this sample mission. Of the ten flight vibration data channels measured and processed, nine provided valid data. Two channels were larger which is likely associated with internal structural responses. The other seven

DFARS 252.235-7010 Acknowledgment of Support and Disclaimer (MAY 1995). (a) This material is based upon work supported by the Naval Surface Warfare Center – Port Hueneme Division (NSWC PHD) Contracting Office under Contract No. N00178-19-D-5001. (b) The opinions, findings, conclusions, and recommendations expressed in this material are those of the authors and do not necessarily reflect the views of the NSWC PHD Contracting.

were very similar. There is some variance between thrust axis and lateral axis measurements. Using all the channels, an average proportionality constant for the mission was computed. This value is consistent with the ratio for other sounding rocket missions.

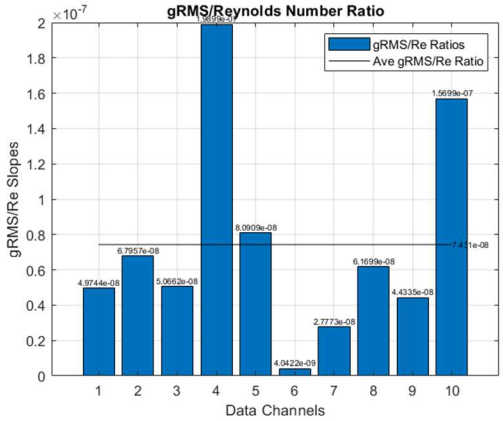

Figure 24. gRMS/Re for Other Data Channels

Vehicle diameters from 14 to 22 inches have been evaluated. L/D ratios of 14 to 28 have been used. Flight trajectories from low/slow single stage vehicles through fast/high four stage vehicles have been considered. All payloads were of a traditional sounding rocket turned skin/joint and deck/longeron construction approach. The gRMS/Re ratios across them all have been consistent. Work continues to re-process older mission data sets to bring them into alignment with the more current analysis processes. New missions are being processed after their flights and the results added to this population.

Another means for looking at the gRMS/Re trend across vehicles is to consider ordered pairs of ratios for thrust axis and lateral axis vibration. Across the sounding rocket missions currently processed, there are 58 ordered pairs of gRMS ratios as shown below. Each grouping of similar vehicles is identified with a different color. The scatter is somewhat broad, but there are distinct patterns. In the plot, the main diagonal line is the line of symmetry where the gRMS/Re ratio for the thrust axis is the same as for the lateral axis. This is where the vibration levels would be isotropic and the same in all directions. The upper diagonal line reflects cases where the lateral vibration is twice as large as the thrust vibration. The lower diagonal shows chases where the lateral vibration is one-half of the thrust vibration. The small radius dotted line is the isobar where the gRMS/Re value is a constant $1x10^{-7}$ gRMS per unit Re. The other two radii reflect a constant ratio of $2x10^{-7}$ and $3x10^{-7}$ gRMS/Re respectively.

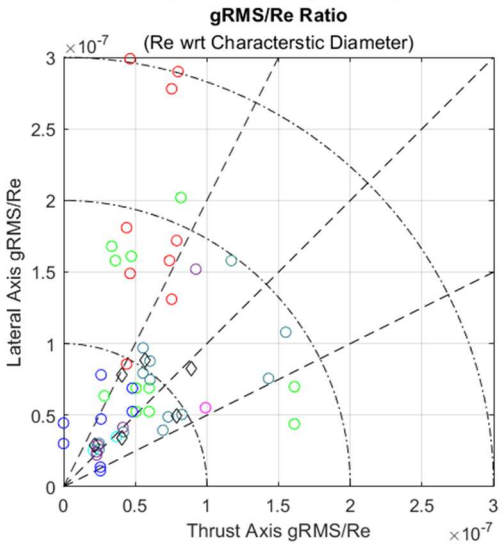

Figure 25. gRMS/Re Across Many Vehicles

At face value, lateral vibration would seem to be about twice the thrust vibration based on this data. However, that trend is heavily influenced by the green and red sets of missions that both had an uncharacteristic Outer Mold Line (OML) geometry and a very high lateral vibration response. That OML would be considered outside the dimensional similarity assumption stated earlier. When those missions are excluded from the population, the trend is for a more equal vibration level in both axes of motion. There are a few data points where the lateral vibration is about half of the thrust axis vibration. It is very possible that these data channels were mis-label in telemetry or crossed in the analysis process. They are plotted faithfully as they were identified, but clearly look like they could have been on the other side of the line of symmetry.

Most missions have a gRMS/Re proportion below $1x10^{-7}$. A smaller subset of missions has a gRMS/Re ratio less than the other contours. Again, it is noted that those missions are the same unusual OML shape missions with the very high lateral vibration levels.

Note also that, the Re for these results is computed using the payload diameter for these results. Payload

DFARS 252.235-7010 Acknowledgment of Support and Disclaimer (MAY 1995). (a) This material is based upon work supported by the Naval Surface Warfare Center – Port Hueneme Division (NSWC PHD) Contracting Office under Contract No. N00178-19-D-5001. (b) The opinions, findings, conclusions, and recommendations expressed in this material are those of the authors and do not necessarily reflect the views of the NSWC PHD Contracting.

diameter is more consistent than total vehicle length, since there are only a few common diameters in use across almost all sounding rocket class vehicles. When the gRMS/Re analysis is performed using total length by stage as the characteristic dimension (as was done for this sample mission), the results have to be rescaled by the L/D ratio to fit the older missions in the population. These data points are shown with diamond markers instead of circles. As the older mission data is re-process and as new mission data is added, the need to make this correction will diminish.

Conclusions

The use of the enhanced Reynolds number approach that includes the RSS vector sum of longitudinal flow Re value and cross flow Re value components, which in turn takes into consideration vehicle instantaneous AoA and DoF atmospheric conditions has been shown to be a superior match to flight vibration gRMS levels. The resulting gRMS/Re ratios for thrust axis and lateral axis vibration have been shown to be consistent across most all other classes of sounding rocket vehicles. Work continues to process older mission data sets using these newer methods and to process more recently flown missions.

For the purposes of estimating the potential gRMS vibration magnitude for a future mission and to have some conservatism and factor of safety in the estimates, one can use the proportionality constant of $2x10^{-7}$ gRMS per unit Re. This can be applied to the vector of Re values predicted for a future mission and based on the characteristic diameter of the payload. Additional cases where this prediction is made in advance of the flight, and then flight vibration data is processed to confirm these gRMS level predictions is recommended. This would represent a better blind assessment of the method and its value.

Acknowledgements

The author would like to thank the following people for their contribution to this body of analysis. Mr. Troy Gammill (NSWC) and Mr. D.C. Pham (NSWC) for providing Navy flight vibration data to enable this analysis. The MDA Tech Team for the sanitized Best Estimate Trajectory data. Dr. Greg McGowen (Corvid Technologies) aerodynamics consultation. Mr. David Lorenzi (Corvid/WSMR Met Group) for balloon measurement data. Mr. Rob Maddox (Peraton) for access to legacy flight vibration data. Mr. Chuck Brodell (NASA) for providing NASA flight vibration data and trajectory data. Mr. Andrew Blazek (Kratos) for other post flight trajectory and wind data. The author would also like to acknowledge the following people for their insights and contributions to this research over the years. Mr. Mark Simko and Mr. Michael Papavisas for trajectory insights. Mr. Charles Lankford, Mr. Jim Diehl, Mr. Hector Parada, and Mr. David Brooks for telemetry and filtering insights. Mr. Jordan Rohanna for signal processing insights.

References

Stanfield, R.W., *Assessment of Flight Vibration versus Reynold's Number for Black Brant IX Sounding Rockets*, 90th SAVE Shock and Vibration Symposium, Atlanta Georgia, November 2019.

Stanfield, R.W., *Trending of Sounding Rocket Flight Vibration with Reynold's Number*, 89th SAVE Shock and Vibration Symposium, Dallas Texas, November 2018.

Stanfield, R.W., *Statistical Compilation and Trending of Sounding Rocket Flight Vibration Environments,* 88th SAVE Shock and Vibration Symposium, Jacksonville, Florida, October 2017.

Stanfield, R.W., *Sounding Rocket Flight Vibration and the Derived Environmental Test Criteria*, ITEA System of Systems Conference, El Paso, Texas, July 2013.